Early-age monitoring of cement-microcement compositions: combined evaluation of chemical reaction and viscoelastic changes during the hardening

Monitoramento da idade inicial de composições de cimento-microcimento: avaliação combinada de reação química e alterações viscoelásticas durante o endurecimento

José Augusto Ferreira de Mesquita 🕛 Marcel Hark Maciel 🗓 Thiago Ricardo Santos Nobre 🗓 Roberto Cesar de Oliveira Romano 🗓 Rafael Giuliano Pileggi 🗓

Abstract

nhancing cement efficiency in concrete and mortar is crucial for reducing the environmental impact of construction by minimizing binder consumption without compromising performance. This study examines the reaction kinetics and hardening of pastes made with two types of Portland cement, each with distinct particle size distributions and mineralogical characteristics. The chemical contribution to hardening was monitored using isothermal calorimetry, while in-situ X-ray diffraction was used to monitor the formation of hydrated compounds. Physical changes were assessed by oscillatory rheometry, focusing on the elastic storage modulus (G'). The detected proportions of portlandite and ettringite influenced the initial reaction stages but had little effect on heat release. The combined analysis reveals the correlation between physicochemical parameters and microstructural changes, emphasizing their role in agglomeration and flocculation forces that accelerate paste hardening.

Keywords: Microcement. Portland cement. Chemical reaction. In-situ X-ray diffraction. Viscoelasticity.

¹José Augusto Ferreira de Mesquita

¹Universidade de São Paulo São Paulo - SP - Brasil

²Marcel Hark Maciel ²Universidade de São Paulo São Paulo - SP - Brasil

³Thiago Ricardo Santos Nobre

3Universidade de São Paulo São Paulo - SP - Brasil

⁴Roberto Cesar de Oliveira

⁴Universidade de São Paulo São Paulo - SP - Brasil

⁵Rafael Giuliano Pileggi

⁵Universidade de São Paulo São Paulo - SP - Brasil

Recebido em 04/06/24 Aceito em 06/09/24

Resumo

A eficiência do cimento em concretos e argamassas é crucial para reduzir o impacto ambiental da construção, minimizando o consumo de ligante sem comprometer o desempenho. Este estudo avalia a cinética de reação e o endurecimento de pastas produzidas com dois tipos de cimento Portland, cada um com distintas distribuições de tamanho de partículas e características mineralógicas. A contribuição química para o endurecimento foi monitorada por meio de calorimetria isotérmica, enquanto a formação de compostos hidratados foi acompanhada por difração de raios X in situ. As alterações físicas foram avaliadas por reometria oscilatória, com foco no módulo de armazenamento elástico (G'). As proporções de portlandita e etringita detectadas influenciaram as etapas iniciais da reação, mas tiveram pouco efeito na liberação de calor. A análise combinada revela a correlação entre os parâmetros físico-químicos e as mudanças microestruturais, destacando seu papel nas forças de aglomeração e floculação que aceleram o endurecimento das pastas.

Palavras-chave: Microcimento. Cimento Portland. Reação química. Difração de raios X in-situ. Viscoelasticidade.

Introduction

To reduce the carbon footprint of the Portland cement industry, several key strategies have emerged. One major approach is the partial replacement of cement with supplementary cementitious materials (SCMs) such as blast furnace slag, fly ash, limestone, silica fume, and others (Guo; Yang; Xiong, 2020; Lothenbach; Scrivener; Hooton, 2011; Schröfl; Gruber; Plank, 2012; Soliman; Tagnit-Hamou, 2017). More recently, limestone calcined clay cement (LC3) (Scrivener *et al.*, 2018; Sharma *et al.*, 2021) is also being used as an option to reduce emissions. Another approach focuses on producing more efficient cement to enhance strength and durability without SCMs, thereby grinding or doping process to improve structural performance and reduce overall material consumption (Liu *et al.*, 2021).

Reducing the porosity of cementitious materials is essential for enhancing performance since porous are directly correlated with mechanical strength and durability. Decreasing porosity can be achieved by reducing water demand and optimizing particle packing (Damineli; Pileggi; John, 2017), enabling the production of high-performance concrete (HPC) and ultra-high-performance concrete (UHPC) (Bajaber; Hakeem, 2021; Yoo; Oh; Banthia, 2022).

Ultrafine particles, such as silica fume and limestone powder, are typically used to fill interparticle voids, increasing packing density and affecting the hydration efficiency (Oey *et al.*, 2013). At this way, less clinker consumption can improve the mechanical strength of eco-efficient materials (Liu *et al.*, 2021; Zheng *et al.*, 2020).

Literature also focuses on techniques to improve the reactivity and efficiency of binders, such as using or modify a grinding process. For example, Liu *et al.* (2021) applied a grinding process to enhance reactivity and, when combined with limestone, it improved the eco-efficiency of the system. However, this process can affect the crystals in the anhydrous material producing higher contents of amorphous (Scrivener *et al.*, 2016) and there still are questions about how this process affects the hardening.

Regardless of SCM addition or grinding process is used, the synergistic blending of different types of cement with distinct physicochemical and mineralogical characteristics offers a promising alternative for optimizing composite binders (Guo; Yang; Xiong, 2020; Liu *et al.*, 2021; Oey *et al.*, 2013; Zheng *et al.*, 2020). When the additions are reactive, such as slags, they directly affect the reaction kinetics (Gruyaert; Robeyst; De Belie, 2010). In the case of inert materials, the physical characteristics of the particles can promote microstructural densification due to the filler effect, facilitating nucleation and accelerating hydration (Arora *et al.*, 2018).

Consequently, the morphology of the formed hydrates increases the surface area and the attraction forces between the particles, influencing the hardening of cementitious suspensions (Fourmentin *et al.*, 2015; Maciel; Romano; Pileggi, 2023). These strategies optimize binder utilization and produce eco-efficient compositions that achieve comparable strength with reduced binder content (Lothenbach; Scrivener; Hooton, 2011).

Oscillatory rheometry, controlling the frequency and strain within the linear viscoelastic regime (LVR), provides continuous and accurate monitoring of the hardening (Betioli, 2007; Romano *et al.*, 2013). This method allows for assessing microstructural rigidity (Yuan *et al.*, 2017) without disrupting microstructure formation. Additionally, isothermal calorimetry is used to monitor the heat released during the cement hydration process, and it is correlated with the chemical parameter of hardening. Combining these methods allows a better understanding of the factors impacting microstructure development and a more precise description of the consolidation process (Romano *et al.*, 2017).

It is important to note that monitoring the heat flow by isothermal calorimetry enables a comprehensive understanding of the main stages of hydration, such as dissolution, induction, and acceleration periods. However, simply observing heat flow does not provide information on which hydrated products are being formed or the kinetics between them. It is known that the reaction of silicates intensifies during the acceleration period, while aluminates react more after this period. Additionally, some hydrated products are formed since the contact with water, even though they do not contribute significantly to the heat flow at that stage. Therefore, for a deep comprehension of the chemical reaction, other techniques should be used in parallel, because the viscoelastic properties of the suspensions, which are related to the physicochemical changes in the particles, are continuously altered from the moment when the water is in contact with the powder.

Crystals such as ettringite tend to form within 5 minutes (Huang *et al.*, 2020), and due to a larger specific surface area (SSA), they have more intense impact on agglomeration forces. However, the reaction is directly dependent on the components used, and blending different types of cement to enhance binders can affect the hydrated compounds formation (Snellings *et al.*, 2018a).

So, this paper aims to elucidate the microstructural development of suspensions combining Ordinary Portland Cement (OPC) with a finer Portland cement of different chemical and mineralogical compositions. This study involves a combined assessment of physical and chemical parameters, including hydration kinetics by calorimetry, mineralogical phase analysis by in-situ X-ray diffraction, and hardening stage by oscillatory rheometry.

Materials and methods

Raw materials characterization

Two types of Portland cements were provided by a partner company. The first is an OPC, and the other, due to its finer particle size than conventional cement, was named microcement (MC). It deserves mentioning that this second is not a commercial product.

The particle size distribution was determined using a Helos laser granulometer (Sympatec) with a detection range of 0.1 to 350 μ m. The specific surface area (SSA) was measured through N2 adsorption at 77 K, following the BET method, using a Belsorp Max instrument from BEL Japan. The cements were pre-treated under vacuum at 10-2 kPa and 40 °C for 16 hours using a BELPREP-vac II (BEL Japan). Specific gravity was assessed using gas He pycnometry with a Quantachrome MVP 5DC instrument. Detailed protocols were described in by Rojas-Ramírez *et al.* (2019). The results obtained for this physical characterization are presented in Figure 1 and Table 1.

MC exhibits a higher amount of finer particles than OPC, with a d50 value seven times smaller, indicating the efficiency of the MC grinding process. Additionally, its SSA is approximately three times higher than OPC, potentially influencing the water demand during mixing. The specific gravity of OPC (3.09 g/cm³) is aligned with typical values for high-clinker content cement, while the lower specific gravity of MC reflects the partial replacement of clinker with mineral additions.

The chemical composition of both cements was assessed using X-ray fluorescence (XRF) with a PANalytical Minipal Cement instrument, following ISO/FDIS 29581-2:2009 guidelines for chemical analysis by XRF (Babikian, 1992). The results are presented in Table 2.

Figure 1 - Particle size distribution of both cements. On the left side is presented the discrete distribution, while on the right is presented the cumulative distribution with the indication of d10, d50 and d90

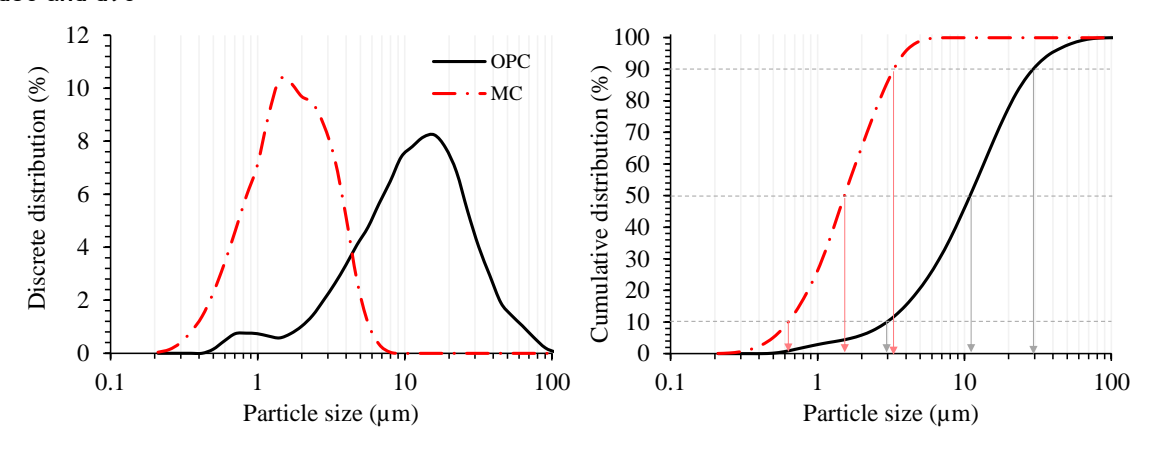


Table 1 - Physical characteristics of cements

Material	d ₁₀ (µm)	d ₅₀ (µm)	d ₉₀ (µm)	SSA* (m ² /g)	Specific gravity (g/cm ³)	VSA** (m ² /cm ³)
OPC	2.81	9.46	26.8	1.26	3.09	3.89
MC	0.59	1.41	2.81	4.03	2.95	11.9

Note: *specific surface area; and **volumetric surface area (product of SSA and specific gravity, indicating the area of particle per volume of powder).

Table 2 - Chemical composition of cements

	SiO ₂	Al ₂ O ₃	Fe ₂ O ₃	CaO	MgO	SO ₃	Na ₂ O	K ₂ O	TiO ₂	P ₂ O ₅	MnO	SrO	LOI
OPC	19.2	4.94	2.97	60.8	0.67	4.47	0.15	0.70	0.25	0.27	0.09	0.27	3.87
MC	30.7	9.79	0.86	42.2	5.66	5.92	0.45	0.60	0.66	< 0.10	0.23	0.07	3.07

OPC contains approximately 60% of CaO and 19% of SiO₂, confirming its high clinker content. The MgO content in both cements complies with the Brazilian standard limit of less than 6.5%, with OPC presenting significantly lower MgO than MC.

The literature indicates that the grinding process does not change the chemical composition but can affect the structure of anhydrous crystals (Iwaszko; Zawada; Lubas, 2018). The chemical profile of MC, with lower CaO and higher SiO₂ contents, suggests it is not clinker-rich and likely includes supplementary cementitious material. The loss on ignition (LOI) for both types of cement was according to Brazilian standards (less than 4.5% for the purest cement). Most of this value refers to carbon dioxide (CO2); the other part is to combined water from the sulfate source and possible pre-hydration. On the other hand, the level of SO₃ for the MC was higher than the limit established by the Brazilian standards, illustrating that this is a kind of special cement. It must be clear that this is not commercial cement and, maybe, due to the large number of finer particles, this excess of sulfate was added for better control of setting time.

Thermogravimetric analysis (TG) was performed to complete the chemical evaluation using a TG 209 F1 Libra equipment (NETZSCH). Around 50 g of cement was placed in an alumina crucible without a lid, heating it from room temperature to $1000~^{\circ}$ C at $10~^{\circ}$ C/min rate, under an inert nitrogen (N2) atmosphere, with a 20 ml/min gas flow. The same test protocol was applied to evaluate the suspension characteristics after hydration stoppage.

The result for the anhydrous cements is shown in Figure 2. The TG/DTG characterization of OPC is typical for this kind of binder, showing mass loss associated with the decomposition of water from portlandite and CO2 from CaCO3. For MC, the analysis reveals a more complex system due to its mineral addition. Notably, brucite decomposition, arising from the MgO in the periclase present in the cement or as a mineral addition, confirms the chemical analysis findings of high MgO content. Additionally, a significant peak observed above 800 °C corresponds to the devitrification of slag into melilite and merwinite, highlighting its unique thermal behaviour (Lothenbach; Durdziński; de Weerdt, 2016). Slag was added to MC because it is speculated that its hardness may increase the efficiency of the grinding process.

Figure 3 illustrates the mineralogy of the anhydrous cements, obtained using X-ray diffraction with a PANalytical Empyrean equipment. Scanning from 5° to 45° 2θ at a step size of 0.02° every 100 seconds was the protocol used. The results for OPC are shown on the left, while those for MC are displayed on the right.

All the clinker phases were observed in both cements. Gypsum (G), bassanite (B), and anhydrite (N) were detected as sulphate phases, with the last one being observed only in MC due to the grinding process, which contributed to the dehydration of gypsum and bassanite. Dolomite (D) was observed in MC, while calcite (C) was present in OPC. Both cements showed evidence of slight pre-hydration, as indicated by the detection of portlandite (P). Finally, MC was found to contain approximately 80% of amorphous material, and the phases gehlenite and merwinite were detected, confirming that it is a special cement with slag addition.

The significant volume of the amorphous in MC is primarily attributable to the mineral additions of slag and the grinding process. It is important to note that excessive grinding, which generates high heat, can cause partial dehydration of hydrated minerals in the clinker, altering its mineralogical composition (STRYDOM; POTGIETER, 1999). Some phases in MC, such as alite and belite, were amorphized during the milling process due to the crystal breakage, as observed in other studies (Mucsi; Rácz; Mádai, 2013; Sekulic; Petrov; Zivanovic, 2004).

In summary, the distinct physicochemical and mineralogical properties of both cements could influence the microstructure formation during the hydration process. So, our study aims to elucidate how these changes occurred during the early stages of hydration.

Figure 2 - Thermal decomposition of cement. On the left is the DTG result, indicating the main phases, and on the right is the mass loss, illustrating the residual mass

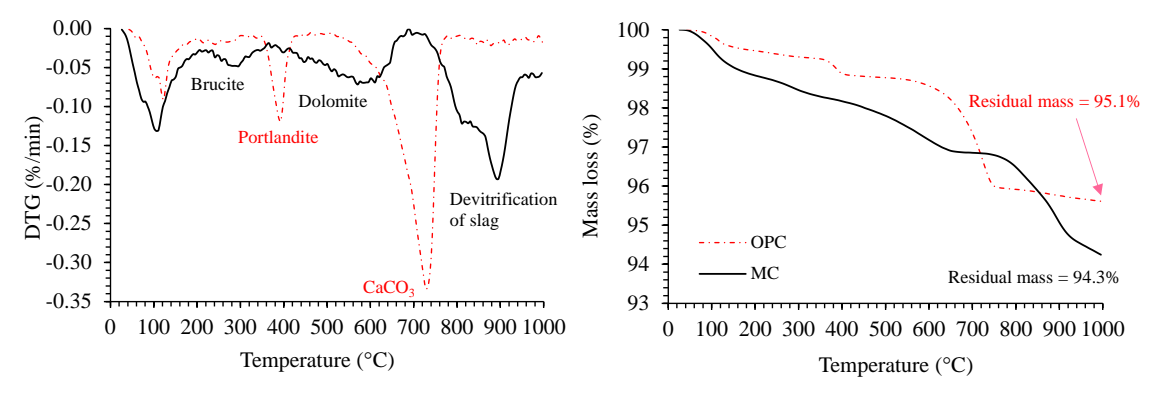
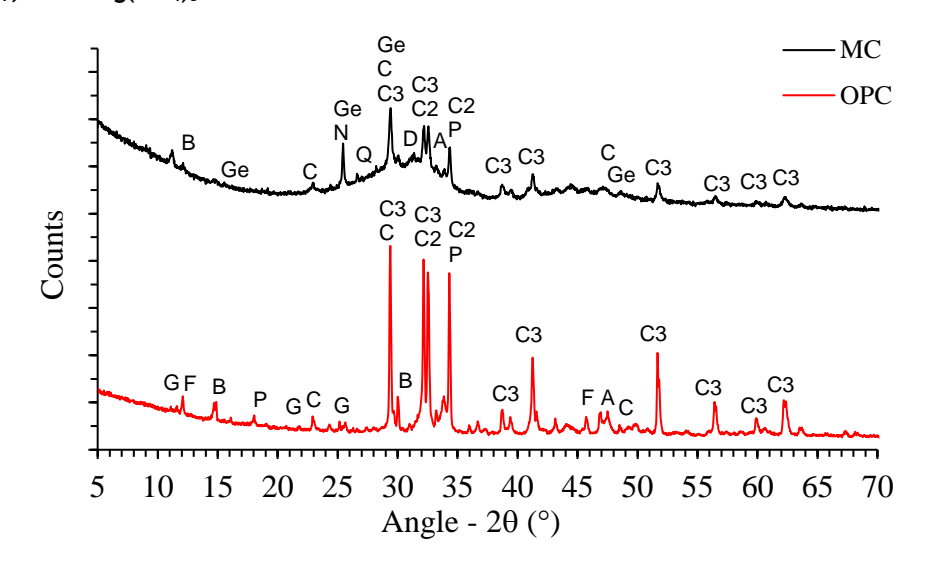


Figure 3 - X-ray diffractograms of both cements - ordinary Portland cement is shown on the left, while MC is displayed on the right - the mineralogical phases are referenced as: $C - CaCO_3$; $C2 - C_2S$; $C3 - C_3S$; C3 - C3S; C3



Mix-design and preparation of suspensions

Cementitious suspensions were prepared with water-to-solid ratio of 0.40, by mass. The OPC was used as a reference, and the other suspensions were partially replaced by 20 and 50% of MC, by volume. No admixtures were used in these compositions to focus solely on evaluating the interaction between different proportions of OPC and MC (from this point of the paper the compositions will be described as xOPC-yMC, where x and y represent the respective proportions of the binders).

Table 3 summarizes the physical characteristics of each composition, including the specific surface area, specific gravity, volumetric surface area, and particle packing (Pof), which were estimated according to the method proposed by Westman and Hugill (1930).

The specific surface area of each composition significantly affects the hydration process and water demand during the mixing. The specific gravity is closely related to the potential for segregation, and the volumetric surface area impacts the efficiency of particle packing and dispersion. This, in turn, influences the number of contact points between the particles, a critical factor in the overall stability and strength of the hydrated binder (Damineli; Pileggi; John, 2017).

Table 3 - Physical characteristics of each composition

-	100OPC	80OPC-20MC	50OPC-50MC		
OPC (in vol-%)	100	80	50		
MC (in vol-%)	-	20	50		
$SSA (m^2/g)$	1.26	1.81	2.65		
Specific gravity (g/cm ³)	3.05	3.03	3.00		
VSA (m²/cm³)	4.31	5.48	7.95		
Pof (%)	17.1	11.3	15.4		

During the mixing process, water was first added to the powder, allowing it to rest for 30 seconds to wet the particles. Subsequently, the mixing was processed in a high-energy shear device, the SpeedMixer by Hauschild, operated at 2,000 rpm for 3 minutes to achieve a homogeneous blend. The suspension obtained was used for rheometry and calorimetry tests.

Methodology for the evaluation of suspensions

Isothermal conduction calorimetry

The kinetic of hydrate formation was assessed using a TAMAir calorimeter maintained at 23 ± 2 °C. After mixing, the paste was immediately sealed in an ampoule, with data collection initializing five minutes postwater addition and for 48 hours.

Fourier Transform Infrared Spectroscopy (FTIR)

Performed at specific hydration intervals (5, 9, and 24 hours) to highlight crucial stages of chemical reactions regarding the cement paste. Samples were prepared to stop hydration through a washing process using isopropanol and, subsequently, diethyl ether, as recommended by the RILEM Technical Committee 238, to reduce the drying temperature. The FTIR spectra were captured using a PerkinElmer Frontier spectrometer equipped with an attenuated total reflectance (ATR) accessory, covering a range of 4000–600 cm-1 at a resolution of 1 cm-1. While the XRD technique assesses crystalline formation, FTIR was mainly used to detect C-S-H formations, aligning observations with key intervals identified in preceding assays (Lodeiro *et al.*, 2009).

Oscillatory rheometry

The viscoelastic properties of the cementitious paste were monitored using a Haake Mars 60 rheometer in a plate-plate geometry. The oscillatory rheometry was assessed over five hours using a time-sweep test, maintaining a constant strain (10-4) and frequency (1 Hz) and employing a solvent trap to minimize evaporation. This technique provided insights into the consistency gain of the suspension over time, reflecting the agglomeration forces, bridge formation, and cohesion (Maciel; Romano; Pileggi, 2023).

In-situ X-ray Diffraction: the in-situ XRD analyses were conducted using a PANalytical Empyrean device. The scans were performed from 5 to 45° 20 at a step size of 0.02° every 100 seconds. The system utilized copper k α 1 radiation (λ = 1.54 Å), with settings of 40 kV voltage and 40 mA current. A Kapton polymeric film and a fixed slit of 1/8° were employed. The in-situ XRD was conducted over 5 hours, with data acquisition every 30 minutes. This allowed for the evaluation of the evolution of CH and Aft phases throughout the hydration process.

Results

Monitoring chemical reaction

In general, the high amorphous volume present in MC makes it difficult to measure the impact on hydration. The degree of reaction of amorphous SCMs remains a challenging task, and a reliable quantification method is still needed (Snellings; Salze; Scrivener, 2014). However, the heat flow is a combination of physical and chemical parameters. Figure 4 illustrates the heat flow and cumulative heat during the hydration of different proportions of cements over the initial 48 hours. This time was chosen for a global comprehension of the kinetic of hydration or different suspensions, to show that there is impact of blends in the main events occurred

in the 2 first days of curing. Table 5 summarises the data depicted in the graph to facilitate comprehension of the results. The times highlighted in the graphic on the left represent some of the main events observed.

The addition of MC did not significantly change the induction period or the reaction rate, quantified up to 5 hours of evaluation, a period close to the setting time defined according to the C1702 (ASTM, 2023). However, notable changes were observed at the 9-hour mark, where the main peak of hydrate formation was lower by increasing MC content. This reduction contradicts expectations from the literature suggesting that ultrafine additions typically enhance hydration (Berodier; Scrivener, 2014), but the dilution of clinker phase can explain the result obtained in this work.

The reaction rate on the acceleration period, influenced by the nucleation and growth of the C-S-H phase, depends on the number of active nucleation points. While the system with MC was expected to exhibit enhanced acceleration due to increased specific surface area, the lower calcium content in 50% MC - about 15% lower - reduced C-S-H precipitation due to a lower Ca/Si ratio despite the increase in nucleation points (Bellmann; Scherer, 2018).

Additionally, the presence of aluminates in MC delayed the hydration process of alite and reduced the formation of hydrated products as the contents of C₃S and C₂S in MC are lower than in pure OPC (Begarin *et al.*, 2011). This effect was less pronounced in the 20% MC mix due to lower dilution and a more dominant physical effect from increased SSA and optimizing the particle packing.

Despite the reduction in heat flow at 9 hours, the heat was increased during the deceleration period from 15 hours onwards. This is attributed to the interaction between soluble aluminates from MC and Ca²⁺ ions from OPC, forming Afm from the Aft phase, thus moderating the peak heat flow based on the concentration of dissociated aluminates.

All the cementitious pastes had its hydration stopped using the RILEM methods (Snellings *et al.*, 2018b) to characterize some hydrated compounds formed and understand the effect of blends on the chemical reaction. Thermogravimetric and FTIR analyses were selected to do this. The times chosen for stopping hydration were based on isothermal calorimetry analyses, focusing on the setting time according to C1702 (5 hours) (ASTM, 2023), maximum peak of silicates and aluminate's reaction (9 hours), and deceleration period, illustrating the beginning of Aft conversion to AFm (24 hours), more intense in the composition with 50OPC-50MC.

Figure 4 - Heat flow and accumulated heat are obtained by calorimetry for each composition - the above is presented over the 48 hours of hydration - in particular, the times of 5, 9 and 24 hours, transition periods in the calorimetry test, are presented

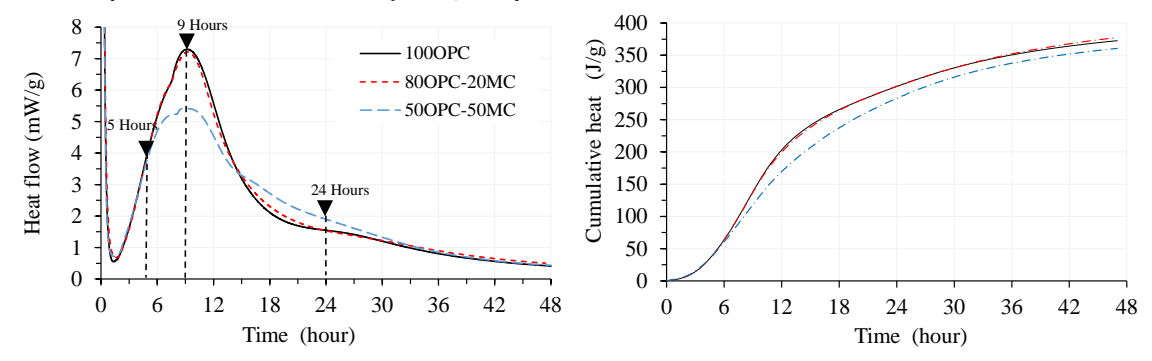


Table 5 - Summary of the main events of chemical reaction

-	100OPC	80OPC-20MC	50OPC-50MC
Beginning of induction period (hour:min)	00:55	00:55	00:55
Time on the induction period (hour:min)	01:00	00:54	01:00
Reaction rate on the acceleration period (mW.g/h)	0.039	0.040	0.042
Time of acceleration period (hour:min)	07:10	07:15	07:10
Setting time according to C1702 (ASTM, 2023)	05:30	05:30	05:25
Heat flow in main peak * (mW/g)	7.3	7.2	5.4
Time to achieve the main peak (hour:min)	09:10	09:05	09:00
Cumulative heat after 48 hours (J/g)	371	376	359

Note: *maximum peak during silicate and aluminates formation, like C-S-H, CH, and Aft

Thermogravimetric analysis

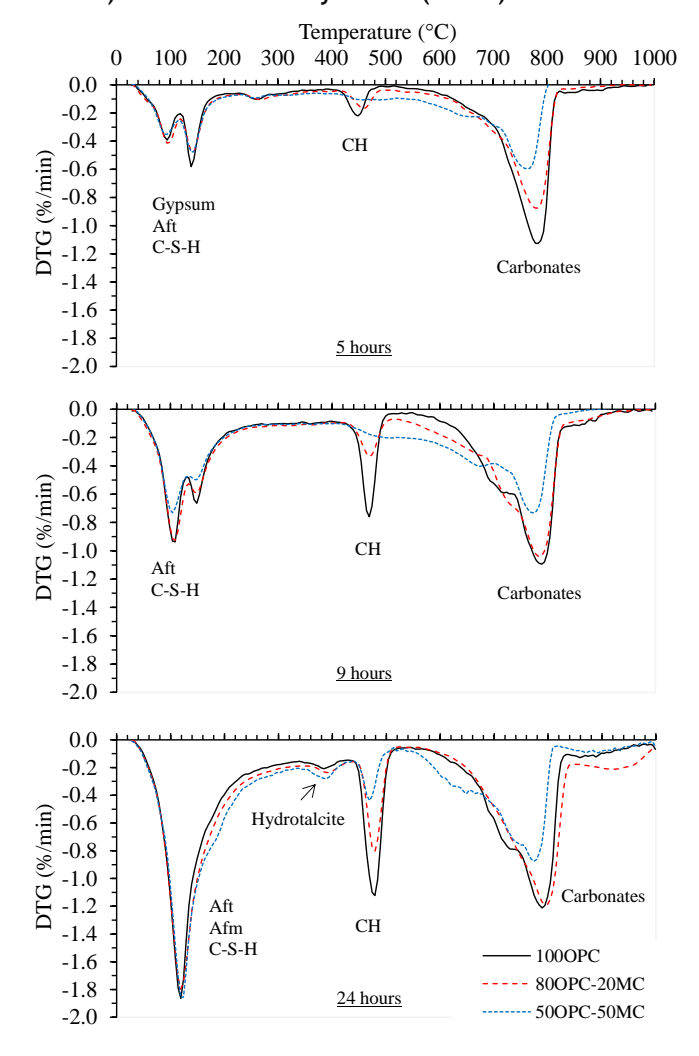
After the hydration stoppage at the times described above, the evaluation of thermal decomposition in each sample was performed. Figure 5 shows the result obtained. In each graphic is presented a comparison between the compositions 100OPC, 80OPC-20MC and 50OPC-50MC for each time of hydration. Above are the results for 5 hours, in the middle for 9 hours and below, for 24 hours, representing the specific events observed by isothermal calorimetry.

In the initial period of 5 hours, it is observed that the content of MC does not significantly impact the formation of ettringite or the consumption of gypsum. However, there is a notable impact on the formation of portlandite. Additionally, for all the compositions, there is a decrease in the carbonate peak relative to the increase in MC content, due to its content in the anhydrous cement.

After 9 hours of reaction, the formation of Aft and C-S-H can be observed more clearly, in addition to the intensification of the formation of portlandite, especially in the compositions with a higher amount of OPC. The beginning of carbonate precipitation can also be observed.

The results at 24 hours are particularly interesting; despite some peak overlap, it is evident that the addition of MC does not significantly affect the formation of C-S-H. Moreover, it is clear a peak corresponding to hydrotalcite, resulted from the milling slag added in the anhydrous product. The thermal decomposition up to 300 °C representing also the formation of Aft and Afm. In the last case, a slightly greater mass loss was observed in the composition with the highest amount of MC.

Figure 5 - Monitoring the hydrated and carbonated phases in the compositions after chemical reaction by 5 (above) 9 (in the middle) and 24 hours of hydration (below)



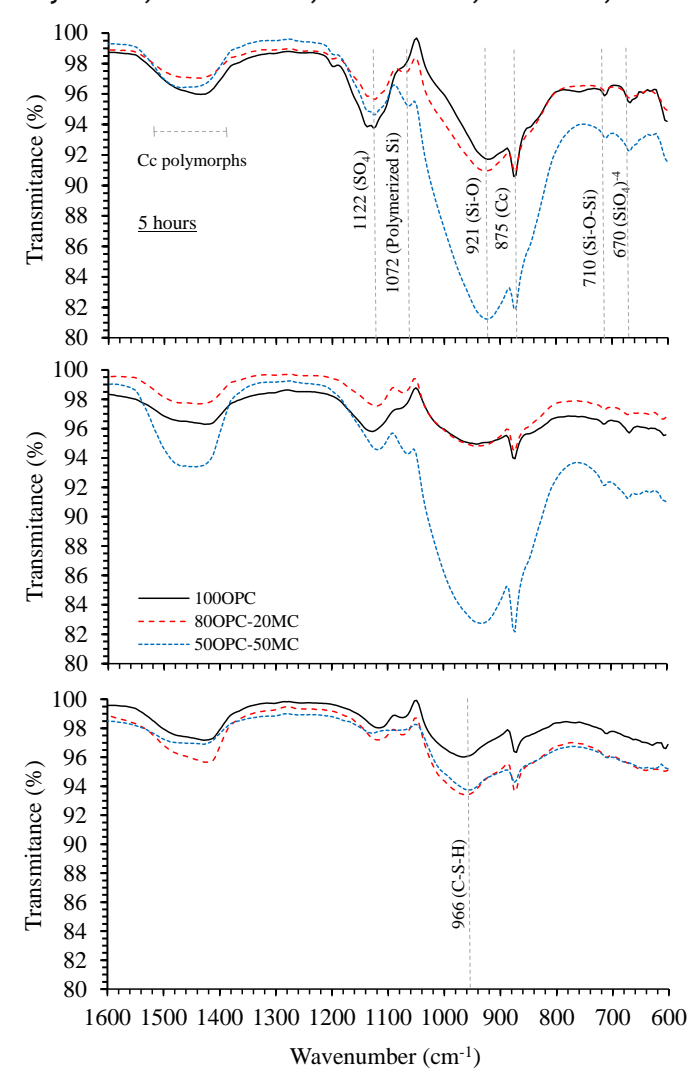
Monitoring C-S-H formation using Fourier Transform-Infrared

Overall, the calorimetric analysis revealed that over a more extended hydration period, MC behaves similarly in the hydration process and formation of hydrated compounds, such as C-S-H formation. However, the C-S-H peak observed at 24 hours may also result from overlapping other hydrated compounds. Therefore, the FTIR assay was conducted to assess the formation of C-S-H more accurately (Yu *et al.*, 1999).

The FTIR spectra of cement blends at various stages of hydration shows changes over time. The addition of MC resulted in an increase in the peak intensities at SiO wavelengths, reflecting the higher silicate content in MC as verified by XRF analysis. Despite this, the substitution of OPC by MC within the first 24 hours did not introduce any new peaks, suggesting a similarity in the initial chemical reactions between the compositions (Figure 6).

Significant changes were observed over time. The decrease in the peak intensity at 1122 cm⁻¹, assigned to sulphate, corresponds to the dissolution of gypsum (Yu *et al.*, 1999). The sharp peak at 875 cm⁻¹ and the broad peak between 1550-1350 cm⁻¹, attributed to carbonates added as additions in the cement, also decreases as hydration progresses and it is in accordance with literature (Reig; Adelantado; Moreno, 2002). A notable shift in peaks between 921-966 cm⁻¹, associated with silica polymerization into C-S-H, indicates that the compositions containing MC show more intense peaks compared to those with pure OPC, suggesting a faster formation of C-S-H in the blends containing MC. The decrease in peaks at 670 cm⁻¹ and 710 cm⁻¹, assigned to the SiO₄⁴⁻ tetrahedra, further supports the occurrence of silica polymerization (Yu *et al.*, 1999).

Figure 6 - Using of FTIR to show the C-S-H formation in the blends of cements - above is presented the result after 5 hours of hydration, in the middle, after 9 hours, and below, after 24 hours



These observations underscore that although calorimetric changes in the heat flow are minimal during the first 5 hours, the formation of hydrates is substantially altered. MC affects the hydration kinetics and enhances the hydrated compounds physicochemical properties, facilitating more extensive polymerization and a more robust formation of C-S-H over time.

The aim so far has been to show that MC can cause a change in the chemical reaction of the blends, forming a greater amount of C-S-H and Aft/Afm, but it was observed that this intensification occurred for the longer reaction times.

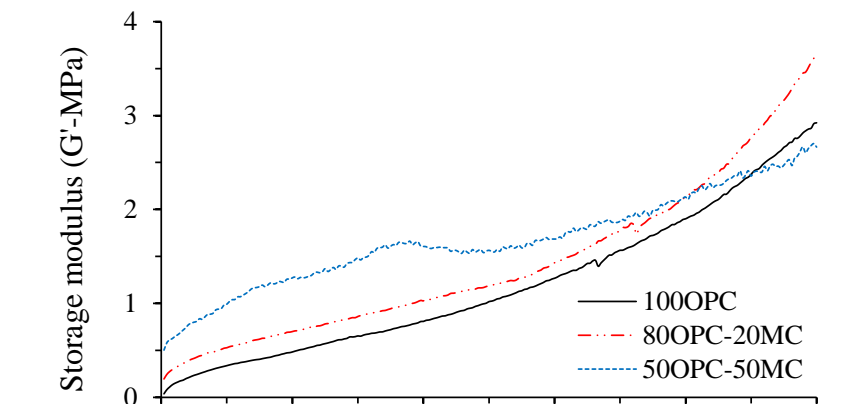
On the other hand, the hardening of the compositions suffered considerable changes up to 5 hours of evaluation, as will be shown below, but with no significant change in the heat flow up to the setting time (close to 5 hours for all the blends). In other words, despite the chemical analyses about the binder efficiency represent a great information about the hardening, do not have neglect the impact in the transition fluid-solid in the first hours of the consolidation, moment that microstructure is being formed.

To evaluate transition from the fluid behaviour to the solid, different researchers work to measuring the viscoelasticity continuously along hydration (Betioli, 2007; Maciel; Romano; Pileggi, 2023; Romano *et al.*, 2017). Most of these studies associated the combination between chemical reaction and the stiffening along the first hours of consolidation. Maciel, Romano and Pileggi (2023) proposed that viscoelasticity depends on the intensity of attraction forces, separating it in agglomeration, flocculation and bridging. So, despite these three variables being adopted with continues, it is possible one of these performs better than others.

Due to the fact that MC had a high SSA and contributes for a better particle packing, the agglomerations forces tend be more predominant than other systems. This paper proposed the application of oscillatory rheometry with time sweep test to monitor the G' evolution, without breaking the microstructure along hydration. To simulate the hardening, during the test the suspension must be into the linear viscoelasticity regime (LVR). This is an important point to correlate the isothermal calorimetry, where the system was in rest along of hydration.

Evaluating the hardening process

The time sweep test measures the evolution of viscoelastic properties in cementitious materials, focusing on the storage modulus (G') during early hydration. Initially, G' is low, reflecting a fluid-like state. As hydration progresses and the material gains rigidity, G' steadily increases, signifying the development of a solid structure. The point where G' begins to rise significantly marks the acceleration of the formation of hydration products and the shift to predominantly elastic behaviour. The rate of increase in G' and the curve shape provide insights into hardening kinetics and microstructural development, highlighting differences in hydration dynamics across various compositions. These results are essential for understanding the link between microstructural changes and the behaviour of cementitious systems, aiding in the optimization of formulations for improved hardening performance.



2

Time (hours)

3

4

5

Figure 7 - Storage modulus is function of time during the first 5 hours

0

1

The initial part of this test quantifies the degree/intensity of microstructural stiffening, correlated to the attraction forces (Maciel; Romano; Pileggi, 2023) in cementitious compositions through the gain in the elastic storage modulus (G'). Figure 7 illustrates the viscoelastic transition of cementitious paste over time, focusing on the early age within the first 5 hours, which is the period allowed for analysis during the liquid-solid transition in the cementitious suspensions.

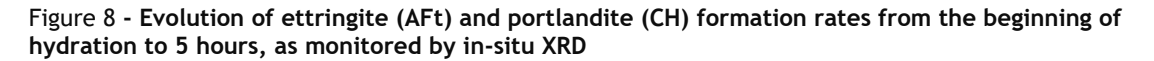
It was observed that the addition of ultra-fines affects the first minutes of hydration mainly due to the initial agglomeration of the cementitious pastes, resulting in a higher initial value of G'. This increase can be attributed to enhanced interparticle forces due to the higher surface area provided by adding microcement (MC), which increased from 1.26 to 2.65 when replaced by 50%. A larger surface area directly influences the initial water demand for particle dispersion, as a greater volume is necessary for wetting and less water available for separating particles. However, as the water content was kept constant, the impact was observed in the rheological parameters. Higher initial values of G' are typically expected in these scenarios, due to the attraction forces, promoting agglomeration, flocculation and bridging, at the same time of the chemical reaction is forming the hydrate compounds (Bentz, 2007; Fourmentin *et al.*, 2015; Maciel; Romano; Pileggi, 2023). This is particularly significant given that each cement type presented distinct particle size distributions and mineralogical compositions.

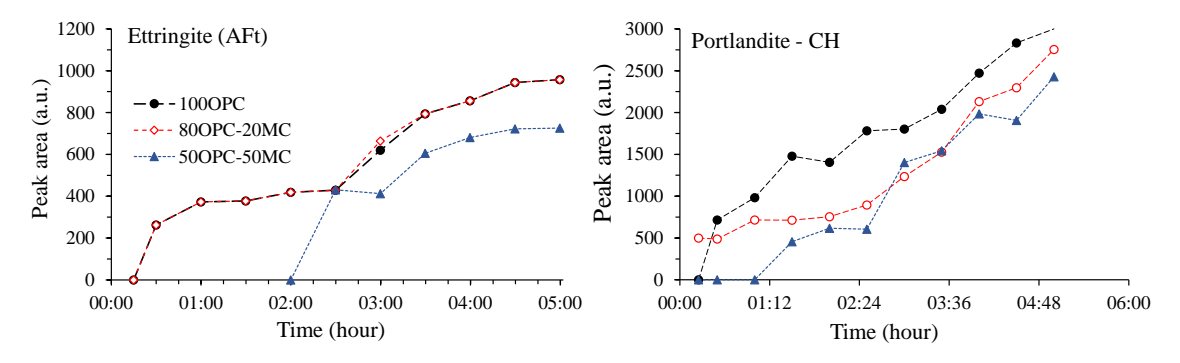
Although the reaction rates between all composition be similar in the first 5 hours of hydration, due to higher clinker content, the 100% OPC composition leads to more intense bond formation among particles during the acceleration period even starting from a less agglomerated system. The reverse occurs in the composition with higher content of microcement, where in the first minutes there was an increase in the rigidify caused by the agglomeration between the particles, while along the hydration the gain is not the same compared to the 1000PC and 80CPV-20MC compositions.

Thus, while there is a consensus that viscoelasticity interacts with cumulative heat (Romano *et al.*, 2017), in this case, the chemical parameter was the same. So, the chemical parameters influenced the viscoelastic transition were not detected using only isothermal calorimetry. In this way, this work is presenting an alternative method to evaluate this combination by focusing on hydrated formation, monitored by in-situ X-ray diffraction.

Although changes in heat flow during the first 5 hours of hydration were not pronounced, in-situ XRD was crucial for understanding the nature of the hydrated products formed during this period. This analysis offers a deeper insight into how MC influences the formation of critical hydrates like CH and AFt, even when heat flow appears stable (De Matos *et al.*, 2022).

To monitor the evolution of ettringite and portlandite formation during the first hours of hydration, the in-situ XRD test was applied. The intensities of peaks corresponding to these hydrates were detected over time, allowing a comparative analysis of their formation. While some theories suggest that this monitoring can be done by summing the areas of all peaks related to the hydrates – such as the peaks at 2θ values of 18.2° , 24° , and 34.5° for portlandite – there is a risk of peak overlap with other phases, which may not represent pure hydrates (Gobbo, 2009). Therefore, in this work, we chose to monitor the isolated peak areas of CH and AFt at 18.2° and 9.06° , respectively, despite the possibility of preferred orientation in some products. Based on this approach, the evolution of crystal formation was monitored, as illustrated in Figure 8.





With the incorporation of MC, the formation of both, ettringite and portlandite, occurs more gradually, with a delay in the process. Specifically, portlandite (CH) detection is delayed by approximately 1.5 hours, while ettringite (AFt) detection is delayed even further by 2.5 hours. This slower precipitation rate is likely due to the significantly reduced content of C_3S in compositions with MC-30 times lower compared to OPC- which impacts the formation of CH and other hydrated compounds (Taylor, 1997).

This observation underscores a crucial point: although calorimetric changes in the heat of hydration are minimal during the first 5 hours, the formation of hydrates is substantially altered. The physicochemical properties of the constituents used profoundly influence the transition fluid-to-solid in cementitious materials. This highlights the importance of combining calorimetry with in-situ XRD for a deep investigation of the hydration process, especially in the early stages.

So, it is clear that MC caused changes in the hardening process of cementitious pastes, both at later ages, in the formation of C-S-H, and at early ages, with the delay in the formation of ettringite and portlandite only during the first 5 hours. To evaluate this process, this stage aimed to assess the combination of physical and chemical parameters in the initial moments. While the high specific surface area (SSA) initially promotes increased attraction forces, the crystal formation process also increases SSA, rigidity, and flocculation, making the fluid-to-solid transition irreversible (even without changes in the cumulative heat).

A combined analysis was performed correlating the gain in microstructural rigidity, analysed through the elastic storage modulus (G') and the kinetics of CH and AFt crystal formation, as shown in Figure 9. This approach enables the assessment of consistency gain considering the amount of these specific hydrates formed.

The results elucidated that there are good correlations between the results, however, each composition followed its own trend, indicating that the formation of portlandite and ettringite impact on the alteration of the forces of attraction, but that other variables also contribute to the stiffening. Independently of that, the intense formation of hydrates directly correlates with the formation of bridges that generate the phenomenon known as bridging between the particles (Maciel; Romano; Pileggi, 2023).

When the formation of CH is considered, an increase in MC content changes the raise of rigidity from an exponential to a linear function, indicating that the gain in microstructural rigidity is less dependent on CH growth in this case. However, the formation of AFt significantly enhances both the initial increase in G' and the intensity of rigidity gain. We see that the evolution is exponential, unlike the same relationship for CH, which is linear. This indicates that the formation of a hydrate with a greater surface area like ettringite, inserted in a suspension with a greater initial surface area, results in a more intense impact on the attraction forces and, consequently, G' increases. This situation also favours particle bridging during hardening.

It is important to mention that the rigidity gain is not solely due to the formation of these two hydrated products but from the entire set of hydrated products formed. Cumulative heat results were used to evaluate this set, estimating the heat released by all formed hydrated products.

Thus, it can be asserted that microstructural gain (G') is related to the type of crystal formed and not solely to the total accumulated heat, as different crystals result in distinct SSAs, which predominantly influence the increase in G'.

In this context, due to its smaller particle size compared to OPC, MC balances the delay induced by dilution effect after the association and increases agglomeration strength from physical components, resulting in a minimally significant impact in the early hours of hydration.

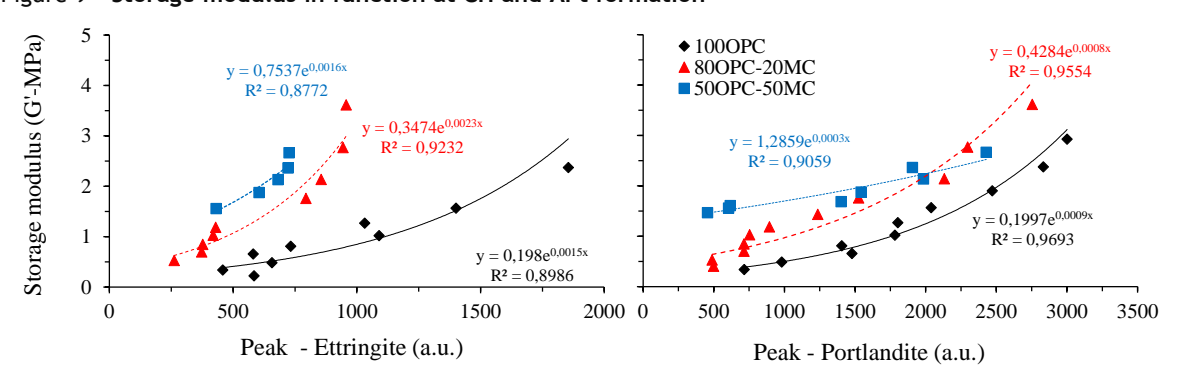


Figure 9 - Storage modulus in function at CH and AFt formation

Conclusions

The study demonstrated that blending different types of cement significantly changes in the chemical reactions during the first 48 hours of hydration. As the proportion of MC increased, a noticeable reduction in heat flow was observed, indicating slower reaction kinetics. Additionally, the presence of MC changed the rate formation of key hydrates like CH, C-S-H, AFt, and AFm. Specifically, higher amounts of MC promoted increased initial formation of AFt, followed by a more pronounced conversion to AFm.

Despite these changes, traditional calorimetry did not detect significant differences during the first 5 hours of hydration — precisely when the paste is transitioning from a fluid to a solid state and the hardening is most rapidly progressing. However, rheological measurements revealed clear changes in viscoelastic properties during this period, highlighting discrepancies between calorimetric data and the actual physical transformations occurring in the material. This change points to the need for a more nuanced understanding of how physical and chemical processes interplay during early hydration.

To understand this gap, we introduced in-situ XRD analysis to monitor the formation of CH and AFt within the first five hours of hydration. This method allowed for direct observation of crystal growth dynamics even in the absence of significant heat flow changes. The results showed that hydrates, particularly CH and AFt, were changed during this period, despite the heat flow by calorimetry be the same. These early formations had a decisive impact on the evolving microstructure, enhancing interparticle attraction forces and influencing the overall hardening process.

The correlation between viscoelastic properties and hydrate formation was great, yet each cement blend exhibited unique trends, suggesting that additional hydrates, beyond CH and Aft, played a role in early hardening. This highlights the complexity of the hardening process, where both the quantity and type of hydrates formed dictate the material's early mechanical behaviour.

Overall, this work advances the understanding of the primary factors that conducted the hardening of cementitious compositions. By integrating in-situ XRD analysis, the study provided a more comprehensive view of the early hydration process, offering valuable insights into the critical role of initial hydrate formation in shaping the mechanical properties of cement-based materials. This approach lays the groundwork for future studies aimed at optimizing cement blends for enhanced performance and sustainability.

Referências

AMERICAN SOCIETY FOR TESTING AND MATERIALS. **C1702**: standard test method for measurement of heat of hydration of hydraulic cementitious materials using isothermal conduction calorimetry. West Conshohocken, 2023,

ARORA, A. *et al.* Microstructural packing- and rheology-based binder selection and characterization for Ultra-High Performance Concrete (UHPC). **Cement and Concrete Research**, v. 103, p. 179–190, jan. 2018.

BABIKIAN, S. H. Raw materials analysis by XRF in the cement industry. **Advances in X-Ray Analysis**, v. 36, p. 139–144, 1992.

BAJABER, M. A.; HAKEEM, I. Y. UHPC evolution, development, and utilization in construction: a review. **Journal of Materials Research and Technology**, v. 10, p. 1058–1074, jan. 2021.

BEGARIN, F. *et al.* Hydration of alite containing aluminium. **Advances in Applied Ceramics**, v. 110, n. 3, p. 127–130, abr. 2011.

BELLMANN; SCHERER. Analysis of C-S-H growth rates in supersaturated conditions. **Cement and Concrete Research**, v. 103, p. 236–244, jan. 2018.

BENTZ, D. P. Cement hydration: building bridges and dams at the microstructure level. **Materials and Structures**, v. 40, n. 4, p. 397–404, may 2007.

BERODIER, E.; SCRIVENER, K. Understanding the filler effect on the nucleation and growth of C-S-H. **Journal of the American Ceramic Society**, v. 97, n. 12, p. 3764–3773, dez. 2014.

BETIOLI, A. M. Influência dos polímeros MHEC e EVA na hidratação e comportamento reológico de pastas de cimento Portland. Florianópolis, 2007. Tese (Doutorado em Engenharia Civil) - Universidade Federal de Santa Catarina, Florianópolis, 2007.

DAMINELI, B. L.; PILEGGI, R. G.; JOHN, V. M. Influence of packing and dispersion of particles on the cement content of concretes. **Revista IBRACON de Estruturas e Materiais**, v. 10, p. 998–1024, 2017.

- DE MATOS, P. R. *et al.* In-situ laboratory X-ray diffraction applied to assess cement hydration. **Cement and Concrete Research**, v. 162, p. 106988, dez. 2022.
- FOURMENTIN, M. *et al.* Porous structure and mechanical strength of cement-lime pastes during setting. **Cement and Concrete Research**, v. 77, p. 1–8, nov. 2015.
- GOBBO, L. de A. **Aplicação da difração de raios-X e método de Rietveld no estudo de cimento Portland**. São Paulo, 2009. Tese (Doutorado em Engenharia Civil) Universidade de São Paulo, São Paulo, 2009.
- GRUYAERT, E.; ROBEYST, N.; DE BELIE, N. Study of the hydration of Portland cement blended with blast-furnace slag by calorimetry and thermogravimetry. **Journal of Thermal Analysis and Calorimetry**, v. 102, n. 3, p. 941–951, dez. 2010.
- GUO, X.; YANG, J.; XIONG, G. Influence of supplementary cementitious materials on rheological properties of 3D printed fly ash based geopolymer. **Cement and Concrete Composites**, v. 114, p. 103820, nov. 2020.
- HUANG, T. *et al.* Understanding the mechanisms behind the time-dependent viscoelasticity of fresh C3A–gypsum paste. **Cement and Concrete Research**, v. 133, p. 106084, jul. 2020.
- IWASZKO, J.; ZAWADA, A.; LUBAS, M. Influence of high-energy milling on structure and microstructure of asbestos-cement materials. **Journal of Molecular Structure**, v. 1155, p. 51–57, mar. 2018.
- LIU, Y. *et al.* Improving environmental efficiency of reverse filling cementitious materials through packing optimization and fiber incorporation. **Molecules**, v. 26, n. 3, p. 647, jan. 2021.
- LODEIRO *et al.* Effect of alkalis on fresh C–S–H gels. FTIR analysis. **Cement and Concrete Research**, v. 39, n. 3, p. 147–153, mar. 2009.
- LOTHENBACH, B.; DURDZINSKI, P.; DE WEERDT, K. Thermogravimetric analysis. A practical guide to microstructural analysis of cementitious materials, v. 1, p. 177-211, 2016.
- LOTHENBACH, B.; SCRIVENER, K.; HOOTON, R. D. Supplementary cementitious materials. **Cement and concrete research**, v. 41, n. 12, p. 1244-1256, 2011.
- MACIEL, M. H.; ROMANO, R. C. de O.; PILEGGI, R. G. Hy_Surf model: viscoelastic evolution in Portland cement suspensions during the early-age hardening. **Cement and Concrete Research**, v. 174, p. 107342, 2023.
- MUCSI, G.; RÁCZ, Á.; MÁDAI, V. Mechanical activation of cement in stirred media mill. **Powder Technology**, v. 235, p. 163–172, fev. 2013.
- OEY, T. *et al.* The filler effect: the influence of filler content and surface area on cementitious reaction rates. **Journal of the American Ceramic Society**, v. 96, n. 6, p. 1978–1990, 2013.
- REIG, F. B.; ADELANTADO, J. G.; MORENO, M. M. FTIR quantitative analysis of calcium carbonate (calcite) and silica (quartz) mixtures using the constant ratio method. **Application to Geological Samples**, Talanta, v. 58, n. 4, p. 811–821, 2002.
- ROJAS-RAMÍREZ, R. A. *et al.* Impacto do uso de resíduo de vermiculita no estado endurecido de argamassas. **Cerâmica**, v. 65, p. 107–116, mar. 2019.
- ROMANO, R. C. de O. *et al.* Evaluation of transition from fluid to elastic solid of cementitious pastes with bauxite residue using oscillation rheometry and isothermal calorimetry. **Applied Rheology**, v. 23, n. 2, abr. 2013.
- ROMANO, R. *et al.* Monitoring of Hardening of Portland Cement Suspensions by Vicat Test, Oscillatory Rheometry, and Isothermal Calorimetry. **Applied Rheology**, v. 27, jul. 2017.
- SCHRÖFL, C. H.; GRUBER, M.; PLANK, J. Preferential adsorption of polycarboxylate superplasticizers on cement and silica fume in ultra-high performance concrete (UHPC). **Cement and Concrete Research**, v. 42, n. 11, p. 1401–1408, nov. 2012.
- SCRIVENER, K. *et al.* **A practical guide to microstructural analysis of cementitious materials**. Boca Raton: CRC Press, 2016.
- SCRIVENER, K. *et al.* Calcined clay limestone cements (LC3). **Cement and Concrete Research**, v. 114, p. 49–56, dez. 2018.

SEKULIC, Z.; PETROV, M.; ZIVANOVIC, D. Mechanical activation of various cements. **International Journal of Mineral Processing**, v. 74, p. S355–S363, dez. 2004.

SHARMA, M. *et al.* Limestone calcined clay cement and concrete: a state-of-the-art review. **Cement and Concrete Research**, v. 149, p. 106564, 2021.

SNELLINGS, R. *et al.* RILEM TC-238 SCM recommendation on hydration stoppage by solvent exchange for the study of hydrate assemblages. **Materials and Structures**, v. 51, p. 1–4, 2018a.

SNELLINGS, R. *et al.* RILEM TC-238 SCM recommendation on hydration stoppage by solvent exchange for the study of hydrate assemblages. **Materials and Structures**, v. 51, n. 6, p. 172, dez. 2018b.

SNELLINGS, R.; SALZE, A.; SCRIVENER, K. L. Use of X-ray diffraction to quantify amorphous supplementary cementitious materials in anhydrous and hydrated blended cements. **Cement and Concrete Research**, v. 64, p. 89-98, 2014.

SOLIMAN, N. A.; TAGNIT-HAMOU, A. Partial substitution of silica fume with fine glass powder in UHPC: filling the micro gap. **Construction and Building Materials**, v. 139, p. 374–383, 2017.

STRYDOM, C. A.; POTGIETER, J. H. Dehydration behaviour of a natural gypsum and a phosphogypsum during milling. **Thermochimica Acta**, v. 332, n. 1, p. 89–96, jul. 1999.

TAYLOR, H. F. Cement chemistry. London: Thomas Telford, 1997.

WESTMAN, A. E. R.; HUGILL, H. R. The packing of particles. **Journal of the American Ceramic Society,** v. 13, n. 10, p. 767–779, 1930.

YOO, D.-Y.; OH, T.; BANTHIA, N. Nanomaterials in ultra-high-performance concrete (UHPC): a review. **Cement and Concrete Composites**, v. 134, p. 104730, 2022.

YU, P. *et al.* Structure of Calcium Silicate Hydrate (C-S-H): near-, mid-, and far-infrared spectroscopy. **Journal of the American Ceramic Society**, v. 82, n. 3, p. 742–748, 1999.

YUAN, Q. *et al.* Small amplitude oscillatory shear technique to evaluate structural build-up of cement paste. **Materials and Structures**, v. 50, n. 2, p. 112, abr. 2017.

ZHENG *et al.* Reverse filling cementitious materials based on dense packing: the concept and application. **Powder Technology**, v. 359, p. 152–160, jan. 2020.

José Augusto Ferreira de Mesquita

Conceptualization, Formal analysis, Investigation, Methodology, Writing - original draft.

Departamento de Engenharia Civil, Escola Politecnica | Universidade de São Paulo | Av. Prof. Almeida Prado, tr. 2, 83 | São Paulo - SP - Brasil | CEP 05508-070 | Tel.: (11) 3091-9170 | E-mail: jose.mesquita@lme.pcc.usp.br

Marcel Hark Maciel

Formal analysis, Writing - review & editing.

Departamento de Engenharia Civil, Escola Politecnica | Universidade de São Paulo | E-mail: marcel.maciel@lme.pcc.usp.br

Thiago Ricardo Santos Nobre

Methodology, Formal analysis.

Departamento de Engenharia Civil, Escola Politecnica | Universidade de São Paulo | E-mail: thiago.nobre@lme.pcc.usp.br

Roberto Cesar de Oliveira Romano

Formal analysis, Writing - original draft.

Departamento de Engenharia Civil, Escola Politecnica | Universidade de São Paulo | Tel.: (11) 3091-5422 | E-mail: rcorjau@gmail.com

Rafael Giuliano Pileggi

Supervision, Writing - review & editing.

Departamento de Engenharia Civil, Escola Politecnica | Universidade de São Paulo | Tel.: (11) 3091-5442 | E-mail: rafael.pileggi@lme.pcc.usp.br

Editor: Enedir Ghisi

Editora de seção: Ana Paula Kirchheim

Ambiente Construído

Revista da Associação Nacional de Tecnologia do Ambiente Construído Av. Osvaldo Aranha, 99 - 3° andar, Centro Porto Alegre - RS - Brasil CEP 90035-190 Telefone: +55 (51) 3308-4084

Telefone: +55 (51) 3308-4084 www.seer.ufrgs.br/ambienteconstruido www.scielo.br/ac

E-mail: ambienteconstruido@ufrgs.br

⊚ 0

This is an open-access article distributed under the terms of the Creative Commons Attribution License.